Mathematical Modelling and Control

https://www.aimspress.com/journal/mmc

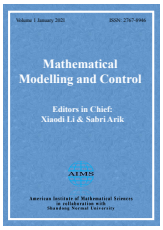

MMC, 5(4): 368–378.
DOI: 10.3934/mmc.2025025
Received: 15 April 2024
Revised: 12 August 2024
Accepted: 09 October 2024
Published: 23 October 2025

Research article

A comparative numerical study and stability analysis of African swine fever virus modelled by Caputo fractional derivative

S. Suganya and V. Parthiban*

Department of Mathematics, School of Advanced Sciences, Vellore Institute of Technology, Chennai - 600127, Tamil Nadu, India

* **Correspondence:** Email: parthiban.v@vit.ac.in.

Abstract: Outbreaks of African swine fever can result in substantial financial repercussions for pig industries in affected areas thereby stemming from the significant mortality rates among pigs and disruptions in the market. In this work, the behavior of an African swine fever virus model with a Caputo fractional derivative is analyzed. The existence and uniqueness results for the proposed fractional order model of African swine fever virus are investigated. The stability of the proposed model is examined within the framework of Ulam-Hyers and generalized Ulam-Hyers. The fractional Adams-Bashforth-Moulton predictor–corrector method is applied to simulate the model, which is compared with the fractional Euler method to validate its efficiency.

Keywords: African swine fever virus; mathematical models; Caputo fractional derivative; Ulam-Hyers stability; numerical simulation

1. Introduction

Fractional calculus has a lengthy history that closely parallels the growth of classical calculus. Fractional calculus has recently been demonstrated to be a successful modeling method for a variety of applications in science and technology ([1, 2]). In the study of numerous infectious diseases, mathematical models play an important role. The fractional epidemic model surpasses classic integer order models as a potent tool for gaining deeper insights into infectious disease dynamics. Comparing it to conventional integer-order models, the use of fractional derivatives in epidemic modeling proves to be more accurate thereby closely aligning with real-world data as evidenced by multiple studies (see [1, 3, 4]). Extensive research have been performed using fractional order differential equations to model epidemiological disease. One of the most prominent usage domains of fractional derivatives is mathematical modeling of diseases in biological investigations. Recently, fractional-order models of biological systems have received a lot of interest (see [3, 5, 6]). This is because, when compared to a classical integer-order model, the fractional model describes the memory and heredity characteristics of the system. There are still many difficult open problems, despite the enormous number of published work on fractional differential equations and dynamical systems.

Agriculture serves as the foundation of rural society and the primary source of income in many countries around the world. The pig farming industry has been expanding quickly since most countries across the world have expanded their meat consumption. The African swine fever virus (ASFV) is one of the greatest threats to pig farming in the world. African swine fever (ASF) has emerged as a formidable challenge for the pork sector thereby causing substantial reductions in pig populations and inflicting severe economic repercussions. It is a contagious and deadly viral disease that affects both domestic and wild pigs worldwide [7]. ASF is caused by an unique virus that exclusively infects domesticated and wild swine, together with a kind of gentle

parasite.

This epidemic disease was first identified in Kenya in 1921, and has remained localized to sub-Saharan African regions [7]. Since then, the disease has spread to numerous African, European, and American countries. Following its containment in Europe by 1999, a resurgence occurred in 2007 when ASFV reemerged in Georgia thus sparking a second epidemic. Rapid transmission ensued, which spanned across Caucasus countries, Russia, and beyond. By 2013, ASF had impacted 22 European nations. The situation worsened in Asia, with the first outbreak reported in China in August 2018 thus triggering significant economic repercussions. Subsequently, ASF proliferated across 18 Asian countries and subsequently reached Oceania and the Americas. Today, ASF continues to pose significant challenges thereby persisting across continents with far-reaching consequences. As a result, the World Organization for Animal Health has classified it as a notifiable illness (OIE). The virus is spread by coming into touch with infected pigs fluids, substances, or corpses of infected pigs. ASF has a variable incubation time; however, it typically lasts between five and fifteen days and and has no effect on people [7]. Because there is no active or artificial vaccination to prevent ASF, the virus must be controlled using rigorous biosecurity measures.

Industrialized swine populations, which are characterized by high animal densities and frequent animal movements, can be particularly susceptible to ASF outbreaks. Effective control strategies for ASF must take the unique challenges posed by these populations into account such as the need for rapid detection and early intervention to prevent the spread of the disease. By understanding the dynamics of ASF within industrialized swine populations, researchers and policymakers can develop targeted control strategies that are tailored to the specific needs and risks of these populations. Recently a small number of integer and non-integer systems have been established to test, investigate, and comprehend the ASF virus (see [1, 5, 8, 9]). In [6], the authors described the integer model for ASFV tranmission dynamics among pigs and ticks. In recent studies, Shi et al. [9] established a non integer model to represent the transmission dynamics of ASF.

The Ulam-Hyers (UH) stability is a well established concept in the field of nonlinear analyses and is widely used to investigate the stability properties of various mathematical models. In recent years, the concept of generalised Ulam-Hyers (GUH) stability has emerged as a powerful tool to study the stability of more complex models. Nevertheless, the application of UH and GUH stability concepts to the ASFV model could provide valuable insights into the long-term behavior of the virus and its potential impact on pig populations. Additionally, it could help identify effective control strategies and inform policy decisions. Therefore, it would be worthwhile for researchers to investigate the stability properties of the ASFV model using UH and generalised UH stability concepts in future studies. Focusing on existing literature, there is a dearth of extensive research on stability analysis of the ASFV model using UH and GUH stability concepts.

Motivated by the preceding studies, this work aims to develop a Caputo sense ASFV model. We utilize the Caputo operator because it has a nonlocal and nonsingular exponential kernel and is best suited to understanding the dynamics of ASFV. In view of the aforementioned discussion, we reconstruct the model in [6] in the Caputo sense using the fractional operator.

The major contributions and novelty of this work are as follows:

- Utilizing a fixed-point theorem, the authors prove the existence and uniqueness of solutions for the ASFV model described by the Caputo fractional derivative.
- Furthermore, a stability analysis of the model solution in the framework of UH and GUH is developed.
- It is crucial to develop numerical techniques to approximate solutions of disease models with minimal computational cost. To achieve this, numerical simulations are conducted that employ the Adams–Bashforth–Moulton Predictor Corrector method (ABM-PECE) to approximate solutions for the proposed model. To assess the reliability of ABM-PECE technique, we perform a comparative analysis with the Fractional Euler Method (FEM). This analysis demonstrates the superior efficiency of the ABM - PECE technique.

The structure of this research article is as follows: in Section 2, basic definitions are discussed; in Section 3, non-

integer order system for ASFV with a Caputo derivative is developed; the existence and uniqueness results of the present model are proven in Section 4; The analysis of stability for the system is performed using UH and GUH in Section 5; a sensitivity analysis of the model is included in Section 6; in Section 7, numerical methods for simulations and discussions are presented; and a conclusion is provided in Section 8.

2. Preliminaries

In this section, the basic definitions of fractional calculus are discussed.

Definition 2.1. *[1] The* **fractional integral of a continuous function** $f(t)$ *on* $L^1([0,T],\mathbb{R})$ *of order* $0 < \zeta \leq 1$ *corresponding to t is defined as follows:*

$$I^{\zeta} f(t) = \frac{1}{\Gamma(\zeta)} \int_0^t (t-s)^{\zeta-1} f(s) ds.$$

Definition 2.2. *[1] The* **Caputo fractional derivative** *of a continuous function* $f(t)$ *on [0, T] is defined by the following:*

$${}^{C}D^{\zeta} f(t) = \frac{1}{\Gamma(n-\zeta)} \int_0^t (t-s)^{n-\zeta-1} \frac{d^n}{dt^n} f(s) ds,$$

where C represents the Caputo derivative, D^{ζ} *denotes the Caputo fractional derivative of order* $n = [\zeta] + 1$*, and* $[\zeta]$ *represents the integer part of* ζ*.*

3. Formulation of Caputo fractional ASFV model

In this study, we redefine the classical model established in [6] into a Caputo fractional order (CFO) model. The CFO model consists of five compartments: susceptible pigs $U(t)$, infected pigs $V(t)$, recovered pigs $W(t)$, susceptible ticks $X(t)$, and infected ticks $Y(t)$.

The CFO derivative system for the ASFV with the parameter $0 < \zeta \leq 1$ is as follows:

$$\begin{cases} {}^{C}D^{\zeta}U(t) = & \bar{\Omega}_P - \bar{\nu}_P U - \bar{\lambda}_1 \frac{UV}{N} - \bar{\lambda}_2 \frac{UY}{N}, \\ {}^{C}D^{\zeta}V(t) = & \bar{\lambda}_1 \frac{UV}{N} + \bar{\lambda}_2 \frac{UY}{N} - (\bar{\nu}_P + \bar{\rho} + \bar{\sigma}) V, \\ {}^{C}D^{\zeta}W(t) = & \bar{\rho} V - \bar{\nu}_P W, \\ {}^{C}D^{\zeta}X(t) = & \bar{\Omega}_T - \bar{\nu}_T X - \bar{\lambda}_3 \frac{XV}{N}, \\ {}^{C}D^{\zeta}Y(t) = & \bar{\lambda}_3 \frac{XV}{N} - \bar{\nu}_T Y. \end{cases} \tag{3.1}$$

Here, N represents the total population of the aforementioned system, and can be written as follows:

$$N = \{U, V, W, X, Y\}.$$

In order to interpret the model, it is assumed that the initial states and all parameters are positive constants. The description of parameters of the proposed model are defined the following Table 1.

Table 1. Interpretation and parameter values (based on [6]).

Parameters	Description	Value
$\bar{\Omega}_P$	Birth rate of susceptible pigs	0.02
$\bar{\Omega}_T$	Birth rate of susceptible ticks	0.2
$\bar{\nu}_P$	Death rate of pigs	0.1
$\bar{\nu}_T$	Death rate of ticks	0.8
$\bar{\lambda}_1$	The proportion of pigs exposed to the virus through contacts with infected pigs	0.4
$\bar{\lambda}_2$	The proportion of pigs that contracted the virus through ticks that were affected	0.2
$\bar{\lambda}_3$	The proportion of ticks that acquired the virus through contact with infected pigs	0.1
$\bar{\rho}$	The proportion of pigs who were virus-free at recovery	0.2
$\bar{\sigma}$	Virus-related death rate	0.3

4. Existence and uniqueness results of Caputo model

This section presents the exitence and uniqueness results of the model (3.1) using the fixed point theory. Consider the model (3.1) in the following form:

$$\begin{cases} {}^{C}D^{\zeta}U(t) = & \mathbb{G}_1(t, U, V, W, X, Y), \\ {}^{C}D^{\zeta}V(t) = & \mathbb{G}_2(t, U, V, W, X, Y), \\ {}^{C}D^{\zeta}W(t) = & \mathbb{G}_3(t, U, V, W, X, Y), \\ {}^{C}D^{\zeta}X(t) = & \mathbb{G}_4(t, U, V, W, X, Y), \\ {}^{C}D^{\zeta}Y(t) = & \mathbb{G}_5(t, U, V, W, X, Y), \end{cases} \tag{4.1}$$

where

$$\begin{cases} \mathbb{G}_1(t,U,V,W,X,Y) = & \bar{\Omega}_P - \bar{\nu}_P U - \bar{\lambda}_1 \frac{UV}{N} - \bar{\lambda}_2 \frac{UY}{N}, \\ \mathbb{G}_2(t,U,V,W,X,Y) = & \bar{\lambda}_1 \frac{UV}{N} + \bar{\lambda}_2 \frac{UY}{N} - (\bar{\nu}_P + \bar{\rho} + \bar{\sigma})\, V, \\ \mathbb{G}_3(t,U,V,W,X,Y) = & \bar{\rho} V - \bar{\nu}_P W, \\ \mathbb{G}_4(t,U,V,W,X,Y) = & \bar{\Omega}_T - \bar{\nu}_T X - \bar{\lambda}_3 \frac{XV}{N}, \\ \mathbb{G}_5(t,U,V,W,X,Y) = & \bar{\lambda}_3 \frac{XV}{N} - \bar{\nu}_T Y. \end{cases} \tag{4.2}$$

Thus, the Caputo model (3.1) takes the following form:

$$\begin{cases} {}^{C}D^{\zeta}\psi(t) & = \mathcal{F}(t,\psi(t)),\ t \in J = [0,b],\ 0 < \zeta \leq 1, \\ \psi(0) & = \psi_0, \end{cases} \tag{4.3}$$

only if

$$\begin{cases} \psi(t) & = (U,V,W,X,Y)', \\ \psi(0) & = (U_0,V_0,W_0,X_0,Y_0)', \\ \mathcal{F}(t,\psi(t)) & = (\mathbb{G}_i(t,U,V,W,X,Y)'),\ i = 1,\cdots,5, \end{cases} \tag{4.4}$$

where $(.)'$ represents the transpose operation. Now, we can write (4.3) by the following integral representation:

$$\begin{cases} \psi(t) = & \psi_0 + \mathcal{J}_0^{\zeta}\mathcal{F}(t,\psi(t), \\ \psi(t) = & \psi_0 + \frac{1}{\Gamma(\zeta)}\int_0^t (t-\upsilon)^{\zeta-1}\mathcal{F}(\upsilon,\psi(\upsilon))d\upsilon. \end{cases} \tag{4.5}$$

Let $\mathbb{S} = C([0,b],\mathbb{R}^5)$ be the Banach space of all continuous functions from [0,b] to $\mathbb{R}^5$ provided with the norm defined by the following:

$$\|\psi\| = \sup_{t\in\mathbb{J}} |\psi(t)|,$$

where $|\psi(t)| = |U(t)| + |V(t)| + |W(t)| + |X(t)| + |Y(t)|$, and $U,V,W,X,Y \in C$.

Assume the following conditions to the nonlinear function $\mathcal{F} \in C([\mathbb{J},\mathbb{R}^5])$and $\mathcal{F} : \mathbb{J}\times\mathbb{R}^5 \to \mathbb{R}^5$ is continuous and bounded in order to determine their existence and uniqueness:

(**A1**) There exists a constants $\Phi \in C\left([0,b],\mathbb{R}^5_+\right) > 0$, $\ni |\mathcal{F}(t,\psi)| \leq \Phi(t)$, for all $(t,\psi) \in \mathbb{J}\times\mathbb{R}^5$; *and*

(**A2**) There exists a constants $\mathcal{L}_{\mathcal{F}} > 0$, $\forall t \in J$ and each $\psi_1(t), \psi_2(t) \in C$, such that

$$|\mathcal{F}(t,\psi_1) - \mathcal{F}(t,\psi_2)| \leq \mathcal{L}_{\mathcal{F}}|\psi_1 - \psi_2|.$$

We apply Krasnoselskii's fixed point theorem to demonstrate the existence of a solution for the system (4.5) that corresponds to the proposed model (3.1).

Lemma 4.1. *([10]) Let* $\mathbf{T}$ *be a closed and convex subset of a Banach space* $\mathbb{S}$*, which is assumed to be* $\mathbf{T} \neq \Phi$*. Take* $\mathbf{P}_1, \mathbf{P}_2$ *as two operators that satisfy the following relations:*
$*\mathbf{P}_1\psi + \mathbf{P}_2\psi \in \mathbf{T}$*, whenever* $\psi \in \mathbf{T}$;
$*$*The operator* $\mathbf{P}_1$ *possesses the properties of compactness and continuity; and*
$*\mathbf{P}_2$ *is a contraction operator.*

Then, there exists $s \in \mathbf{T}$ *such that* $s = \mathbf{P}_1 s + \mathbf{P}_2 s$.

Theorem 4.1. *Given the assumption* (**A1**)*, together with the continuity of* $\mathcal{F}$*, then (4.5) which is equivalent with the mentioned system (3.1), has atleast one solution when*

$$\mathcal{L}_{\mathcal{F}}\,\|\psi_1(t_0) - \psi_2(t_0)\| < 1.$$

Proof. Now, let $\sup_{t\in J}|\Phi(t)| = \|\Phi\|$ and $\eta \geq \|\psi_0\| + \Theta\|\Phi\|$. Additionally, we consider $\mathbf{C}_\eta = \{\psi \in \mathbb{S} : \|\psi\| \leq \eta\}$.

Take two operators $\mathbf{P}_1, \mathbf{P}_2$ on $\mathbf{C}_\eta$ defined by the following:

$$(\mathbf{P}_1\psi)(t) = \frac{1}{\Gamma(\zeta)}\int_0^t (t-\upsilon)^{\zeta-1}\mathcal{F}(\upsilon,\psi(\upsilon))d\upsilon, \quad t \in J,$$

and

$$(\mathbf{P}_2\psi)(t) = \psi(t_0), \quad t \in J.$$

Thus, for any $\psi_1, \psi_2 \in \mathbf{C}_\eta$, yields the following:

$$\begin{aligned} &\|(\mathbf{P}_1\psi_1)(t) + (\mathbf{P}_2\psi_2)(t)\| \\ &\leq \|\psi_0\| + \frac{1}{\Gamma(\zeta)}\int_0^t (t-\upsilon)^{\zeta-1}\|\mathcal{F}(\upsilon,\psi_1(\upsilon))\|d\upsilon, \\ &\leq \|\psi_0\| + \Theta\|\Phi\|, \\ &\leq \eta < \infty. \end{aligned}$$

$\mathbf{P}_1\psi_1 + \mathbf{P}_2\psi_2 \in \mathbf{C}_\eta$.

To show that $\mathbf{P}_2$ is contraction operator, for any $\psi_1, \psi_2 \in \mathbf{C}_\eta$, we obtain the following:

$$\|(\mathbf{P}_2\psi_1)(t) - (\mathbf{P}_2\psi_2)(t)\| \leq \|\psi_1(t_0) - \psi_2(t_0)\|. \tag{4.6}$$

Hence, $\mathbf{P}_2$ is contraction operator. Additionally, the operator $\mathbf{P}_1$ must be continuous because the function $\mathcal{F}$ is continuous. Moreover , for any $t \in J$ and $\psi_1 \in \mathbf{C}_\eta$,

$$\|\mathbf{P}_1\psi\| \leq \Theta\,\|\Phi\| < +\infty. \tag{4.7}$$

Hence, $\mathbf{P}_1$ is bounded uniformly.

To prove the operator $\mathbf{P}_1$, which is closed and bounded, let $\sup_{(t,\psi)\in J\times\mathbf{C}_\eta}|\mathcal{F}(t,\psi(t))| = \mathcal{F}^*$; then, for any $t_1, t_2 \in J$ such that $t_2 \geq t_1$, the following holds:

$$
\begin{aligned}
&|(\mathbf{P}_1\psi)(t_2) - (\mathbf{P}_1\psi)(t_1)| \\
&\quad = \Big|\frac{1}{\Gamma(\zeta)}\int_0^{t_2}(t_2-\upsilon)^{\zeta-1}\mathcal{F}(\upsilon,\psi(\upsilon))d\upsilon \\
&\quad\quad - \frac{1}{\Gamma(\zeta)}\int_0^{t_1}(t_1-\upsilon)^{\zeta-1}\mathcal{F}(\upsilon,\psi(\upsilon))d\upsilon\Big| \\
&\quad \leq \frac{\mathcal{F}^*}{\Gamma(\zeta)}\Big|\int_0^{t_1}[(t_2-\upsilon)^{\zeta-1} - (t_1-\upsilon)^{\zeta-1}]\mathcal{F}(\upsilon,\psi(\upsilon))d\upsilon \\
&\quad\quad + \int_{t_1}^{t_2}(t_2-\upsilon)^{\zeta-1}\mathcal{F}(\upsilon,\psi(\upsilon))d\upsilon\Big| \\
&\quad \leq \frac{\mathcal{F}^*}{\Gamma(\zeta)}\Big(2(t_2-t_1)^{\zeta} + (t_2^{\zeta} - t_1^{\zeta})\Big) \\
&\quad \to 0, as\ t_2 \to t_1.
\end{aligned}
$$

Hence, $\mathbf{P}_1$ is equicontinuous and is relatively compact on $\mathbf{C}_\eta$. By applying the Arzelá Ascoli theorem, $\mathbf{P}_1$ is compact on $\mathbf{C}_\eta$ because the operator is uniformly bounded and continuous. Hence, model (3.1) has at least one solution on $t \in J$ according to the fixed point theorem of Krasnoselskii's. □

Theorem 4.2. *Equation (4.5), which is equivalent with the mentioned system (3.1), has a unique solution under the assumption* (**A2**) *provided that* $\Theta\mathcal{L}_{\mathcal{F}} < 1$, *where* $\Theta = b^{\zeta}[\Gamma(\zeta+1)^{-1}]$.

Proof. Consider $\mathbf{B} : \mathbb{S} \to \mathbb{S}$ defined by the following:

$$
(\mathbf{B}\psi)(t) = \psi_0 + \frac{1}{\Gamma(\zeta)}\int_0^t (t-\upsilon)^{\zeta-1}\mathcal{F}(\upsilon,\psi(\upsilon))d\upsilon. \tag{4.8}
$$

Here, $\mathbf{B}$ is a well defined operator, and the only solution to model (3.1) is merely the fixed point of $\mathbf{B}$. Let $\sup_{t\in\mathbb{J}} \|\mathcal{F}(t,0)\| = \mathbf{A_1}$ and $\mathcal{F} \geq \|\psi_0\| + \Theta\mathbf{A_1}$. Therefore, we show that $\mathbf{B}\mathbb{L}_{\mathcal{F}} \subset \mathbb{L}_{\mathcal{F}}$.

Here, $\mathbb{L}_{\mathcal{F}} = \{\psi \in \mathbb{S} : \|\psi\| \leq \mathcal{F}\}$ is closed and convex. For any $\psi \in \mathbb{L}_{\mathcal{F}}$, we obtain the following:

$$
\begin{aligned}
|\mathbf{B}\psi(t)| &= |\psi_0| + \frac{1}{\Gamma(\zeta)}\int_0^t (t-\upsilon)^{\zeta-1}|\mathcal{F}(\upsilon,\psi(\upsilon))d\upsilon| \\
&\leq \psi_0 + \frac{1}{\Gamma(\zeta)}\int_0^t (t-\upsilon)^{\zeta-1}[\mathcal{L}_{\mathcal{F}}|\psi(\upsilon)| + \mathbf{A_1}]d\upsilon \\
&\leq \psi_0 + \frac{(\mathcal{L}_{\mathcal{F}}\|\psi\| + \mathbf{A_1})}{\Gamma(\zeta)}\int_0^t (t-\upsilon)^{\zeta-1}d\upsilon \\
&\leq \psi_0 + \frac{(\mathcal{L}_{\mathcal{F}}\mathcal{F} + \mathbf{A_1})b^{\zeta}}{\Gamma(\zeta+1)} \\
&\leq \psi_0 + \Theta(\mathcal{L}_{\mathcal{F}}\mathcal{F} + \mathbf{A_1})
\end{aligned}
$$

$$\therefore |\mathbf{B}\psi(t)| \leq \mathcal{F}.$$

For any $\psi_1, \psi_2 \in \mathbb{S}$, we obtain the following:

$$
\begin{aligned}
&|(\mathbf{B}\psi_1)(t) - (\mathbf{B}\psi_2)(t)| \\
&\quad = \Big|\frac{1}{\Gamma(\zeta)}\int_0^t (t-\upsilon)^{\zeta-1}[\mathcal{F}(\upsilon,\psi_1(\upsilon)) - \mathcal{F}(\upsilon,\psi_2(\upsilon))]\Big|d\upsilon, \\
&\quad \leq \frac{\mathcal{L}_{\mathcal{F}}}{\Gamma(\zeta)}\int_0^t (t-\upsilon)^{\zeta-1}|\psi_1(\upsilon) - \psi_2(\upsilon)|d\upsilon, \\
&|(\mathbf{B}\psi_1)(t) - (\mathbf{B}\psi_2)(t)| \leq \Theta\mathcal{L}_{\mathcal{F}}|\psi_1(\upsilon) - \psi_2(\upsilon)|,
\end{aligned}
$$

which implies that $\|(\mathbf{B}\psi_1) - (\mathbf{B}\psi_2)\| \leq \Theta\mathcal{L}_{\mathcal{F}}\|\psi_1 - \psi_2\|$.

As a result of the Banach contraction principle, the proposed model (3.1) has a unique solution. □

Remark 4.1. *Using the Krasnoselskii's fixed point theorem and Banach Contraction principle, the prescribed model has a unique solution.*

5. Analysis of stability

In this section, the UH and GUH stability concepts are used to assess the stability analysis of the Caputo fractional model (3.1) (see [11, 12]). Recently, many authors established UH and GUH stability of a nonlinear fractional models of epidemic diseases such as COVID-19, HIV/AIDS, Tuberculosis, Malaria, Dengue fever, Zika, Ebola, and Hepatitis [13–17]. Let us consider the inequality for $\epsilon > 0$; then,

$$
\Big|D^{\zeta}\bar{\psi}(t) - \mathcal{F}(t,\bar{\psi}(t))\Big| \leq \epsilon, t \in \mathbb{J}, \tag{5.1}
$$

where $\epsilon = max(\epsilon_j)^T$, $j = 1, \cdots, 5$

Remark 5.1. *Consider a function* $\bar{\psi} \in \mathbb{S}$ *as a solution of (5.1) such that if there is a function* $h \in \mathbb{S}$ *and for all t belongs to* $\mathbb{J}$, *then the following conditions are satisfied:*

$$
\begin{aligned}
&(a)|h(t)| \leq \epsilon, h = max(h_j)^T, \\
&(b)D^{\zeta}\bar{\psi}(t) = \mathcal{F}(t,\bar{\psi}(t)) + h(t).
\end{aligned}
$$

Definition 5.1. *[14, 17] The proposed system (3.1) is UH stable if there is* $\kappa > 0$ *such that* $\epsilon > 0$, *and for every solution* $\bar{\psi} \in \mathbb{S}$ *which satisfies (5.1), there exists a solution* $\psi \in \mathbb{S}$ *of (4.3) with*

$$
\Big|\bar{\psi}(t) - \psi(t)\Big| \leq \kappa\epsilon, \quad t \in \mathbb{J},
$$

where $\kappa = max(\kappa_j)^T$.

Definition 5.2. *[14,17] The proposed system (3.1) is said to be GUH stable if there is a continuous function $\phi_{\mathcal{F}} : \mathbb{R}_+ \to \mathbb{R}_+$ with $\phi_{\mathcal{F}}(0) = 0$, such that, for each solution $\bar{\psi} \in \mathbb{S}$ of (5.1), there exists a solution $\psi \in \mathbb{S}$ of (3.1) such that*

$$\left|\bar{\psi}(t) - \psi(t)\right| \leq \phi_{\mathcal{F}}\epsilon, \quad t \in \mathbb{J},$$

where $\phi_{\mathcal{F}} = max(\phi_{\mathcal{F}_j})^T$.

Now, we present the UH stability result of the Caputo fractional order model.

Lemma 5.1. *[14, 17] Assume that $\bar{\psi} \in \mathbb{S}$ satisfies inequality (5.1); then, $\bar{\psi}$ satisfies the following integral inequality:*

$$\left|\bar{\psi}(t) - \bar{\psi}_0 - \frac{1}{\Gamma(\zeta)}\int_0^t (t-\upsilon)^{\zeta-1}\mathcal{F}(\upsilon, \bar{\psi}(\upsilon))d\upsilon\right| \leq \Theta\epsilon.$$

Proof. By condition (b) from the aforementioned remark of (5.1),

$$\bar{\psi}(t) = \bar{\psi}_0 + \frac{1}{\Gamma(\zeta)}\int_0^t (t-\upsilon)^{\zeta-1}\mathcal{F}(\upsilon, \bar{\psi}(\upsilon))d\upsilon + \frac{1}{\Gamma(\zeta)}\int_0^t (t-\upsilon)^{\zeta-1}h(\upsilon)d\upsilon.$$

By condition (a) from the aforementioned remark of (5.1) and hypothesis (**A1**), we obtain the following:

$$\begin{aligned}&\left|\bar{\psi}(t) - \bar{\psi}_0 - \frac{1}{\Gamma(\zeta)}\int_0^t (t-\upsilon)^{\zeta-1}\mathcal{F}(\upsilon, \bar{\psi}(\upsilon))d\upsilon\right| \\ \leq &\frac{1}{\Gamma(\zeta)}\int_0^t (t-\upsilon)^{\zeta-1}|h(\upsilon)|d\upsilon \\ \leq &\Theta\epsilon.\end{aligned}$$

This completes the proof. □

Theorem 5.1. *Suppose that $\mathcal{F} : \mathbb{J} \times \mathbb{R}^5 \to \mathbb{R}^5$ is continuous for every $\psi \in \mathbb{E}$ and hypothesis (**A2**) holds with 1-$\Theta\mathcal{L}_{\mathcal{F}} > 0$. Then, the prescribed system (3.1) is stable in the UH and GUH senses.*

Proof. Assume that $\psi \in \mathbb{S}$ is the only solution to (3.1) and that $\bar{\psi} \in \mathbb{S}$ satisfies inequality (5.1). Hence, for any $\epsilon > 0$, $t \in \mathbb{J}$ and Lemma (5.1) provides the following:

$$\begin{aligned}&|\bar{\psi}(t) - \psi(t)| \\ &= \max_{t\in\mathbb{J}}\left|\bar{\psi} - \psi_0 - \frac{1}{\Gamma(\zeta)}\int_0^t (t-\upsilon)^{\zeta-1}\mathcal{F}(\upsilon, \psi(\upsilon))d\upsilon\right| \\ &\leq \max_{t\in\mathbb{J}}\left|\bar{\psi}(t) - \bar{\psi}_0 - \frac{1}{\Gamma(\zeta)}\int_0^t (t-\upsilon)^{\zeta-1}\mathcal{F}(\upsilon, \bar{\psi}(\upsilon))d\upsilon\right| \\ &\quad + \max_{t\in\mathbb{J}}\frac{1}{\Gamma(\zeta)}\int_0^t (t-\upsilon)^{\zeta-1}\left|\mathcal{F}(\upsilon, \bar{\psi}(\upsilon)) - \mathcal{F}(\upsilon, \psi(\upsilon))\right|d\upsilon \\ &\leq \left|\psi(t) - \bar{\psi}_0 - \frac{1}{\Gamma(\zeta)}\int_0^t (t-\upsilon)^{\zeta-1}\mathcal{F}(\upsilon, \bar{\psi}(\upsilon))d\upsilon\right| \\ &\quad + \frac{\mathcal{L}_{\mathcal{F}}}{\Gamma(\zeta)}\max_{t\in\mathbb{J}}\int_0^t (t-\upsilon)^{\zeta-1}|\bar{\psi}(\upsilon) - \psi(\upsilon)|d\upsilon \\ &\leq \Theta\epsilon + \Theta\mathcal{L}_{\mathcal{F}}\|\bar{\psi} - \psi\|\end{aligned}$$

from which we obtain $\|\bar{\psi} - \psi\| \leq \kappa\epsilon$, where $\kappa = \frac{\Omega}{1-\Omega\mathcal{L}_{\mathcal{F}}}$,
$\therefore |\bar{\psi}(t) - \psi(t)| \leq \kappa\epsilon$.

Thus, the proposed system (3.1) is stable under UH and GUH stability. This completes the proof. □

6. Sensitivity analysis

In this section, a sensitivity analysis is performed to determine which parameters contribute to the basic reproduction number $\mathcal{R}_0$. Based on this strategy, we can determine which parameters contribute to $\mathcal{R}_0$.

Thus,

$$\mathcal{R}_0 = \frac{\bar{\lambda}_1}{\bar{\nu}_P + \bar{\rho} + \bar{\sigma}}.$$

The sensitivity index of the model parameter is given by the relation

$$\Gamma_A^{\mathcal{R}_0} = \frac{\partial\mathcal{R}_0}{\partial A} \times \frac{A}{\mathcal{R}_0}.$$

The sensitivity analysis presented in Table 2 and Figure 1 indicates that the role of various parameters in determining $\mathcal{R}_0$. The results highlight that contacts with infected pigs are the most sensitive parameters thereby leading to a considerable increase in $\mathcal{R}_0$. This suggests that an increase in these contacts will enhance $\mathcal{R}_0$. In contrast, the recovery rate shows a minimal sensitivity thereby implying that raising the recovery rate will reduce $\mathcal{R}_0$.

Table 2. Sensitivity analysis of parameter values.

Parameters	Value	Sensitivity indexes
$\bar{\lambda}_1$	0.4	1
$\bar{\nu}_P$	0.1	-0.1667
$\bar{\rho}$	0.2	-0.3333
$\bar{\sigma}$	0.3	-0.5

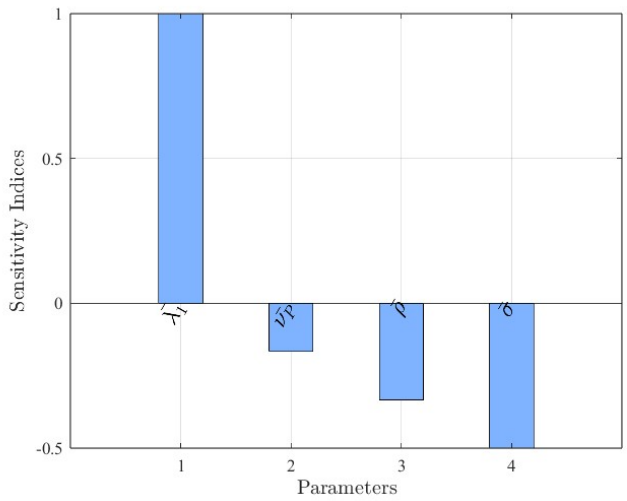

Figure 1. Sensitivity analysis of parameter values.

7. Numerical methods for ASFV model

For various values of the parameters, we provide numerical results to better understand the dynamical behavior of system (3.1). We employ a comparative analysis to evaluate the performance of the fractional ABM-PECE method and FEM. The comparison encompasses various fractional derivative orders and the specific case of the integer order.

7.1. Solution for ASFV model using FEM

The Euler method is the most widely used numerical strategy for any fractional order initial value problem (see [18–22]). To derive the iterative scheme, we shall represent the fractional model (3.1) in a concise and straightforward form as follows:

$$\begin{cases} {}^{C}D_t^{\zeta} f(t) &= \mathbf{F}(t, f(t)), \\ f(0) &= f_0, \quad 0 < \mathbf{T} < \infty. \end{cases} \tag{7.1}$$

Here, we consider a continuous real-valued vector function $\mathbf{F}(t, f(t))$ denoted by $f = (U, V, W, X, Y) \in \mathbb{R}^5$, which satisfies the Lipschitz condition, where f_0 represents the initial state vector. By integrating both sides of (7.1), we arrive at the following result:

$$f(t) = f_0 + \frac{1}{\Gamma(\zeta)} \int_0^t (t-\xi)^{\zeta-1} \mathbf{F}(\xi, f(\xi)) d\xi. \tag{7.2}$$

The numerical simulation of a nonlinear CFO (3.1) is explained using the FEM method. The following is a representation of the algorithm.

Assume $h = \frac{T}{m}, m \in \mathbb{N}, n = 0, \cdots, m.$

$$f_{n+1} = f_0 + \frac{h^{\zeta}}{\Gamma(\zeta+1)} \sum_{j=0}^{n} \Big((n-j+1)^{\zeta} - (n-j)^{\zeta}\Big) \mathbf{F}\Big(t_j, f\left(t_j\right)\Big).$$

Therefore, the FEM formulae for the prescribed system (3.1) takes the following form:

$$\begin{aligned} U_{n+1} =& U_0 + \frac{h^{\zeta}}{\Gamma(\zeta+1)} \sum_{j=0}^{n} \Big((n-j+1)^{\zeta} - (n-j)^{\zeta}\Big) \\ & \Big(\bar{\Omega}_P - \bar{\nu}_P U - \bar{\lambda}_1 \frac{UV}{N} - \bar{\lambda}_2 \frac{UY}{N}\Big), \\ V_{n+1} =& V_0 + \frac{h^{\zeta}}{\Gamma(\zeta+1)} \sum_{j=0}^{n} \Big((n-j+1)^{\zeta} - (n-j)^{\zeta}\Big) \\ & \Big(\bar{\lambda}_1 \frac{UV}{N} + \bar{\lambda}_2 \frac{UY}{N} - (\bar{\nu}_P + \bar{\rho} + \bar{\sigma}) V\Big), \\ W_{n+1} =& W_0 + \frac{h^{\zeta}}{\Gamma(\zeta+1)} \sum_{j=0}^{n} \Big((n-j+1)^{\zeta} - (n-j)^{\zeta}\Big) \\ & (\bar{\rho} V - \bar{\nu}_P W), \\ X_{n+1} =& X_0 + \frac{h^{\zeta}}{\Gamma(\zeta+1)} \sum_{j=0}^{n} \Big((n-j+1)^{\zeta} - (n-j)^{\zeta}\Big) \\ & \Big(\bar{\Omega}_T - \bar{\nu}_T X - \bar{\lambda}_3 \frac{XV}{N}\Big), \\ Y_{n+1} =& Y_0 + \frac{h^{\zeta}}{\Gamma(\zeta+1)} \sum_{j=0}^{n} \Big((n-j+1)^{\zeta} - (n-j)^{\zeta}\Big) \\ & \Big(\bar{\lambda}_3 \frac{XV}{N} - \bar{\nu}_T Y\Big). \end{aligned}$$

7.2. Solution for ASFV model using ABM-PECE method

The ABM-PECE method stands as the predominant numerical technique to solve fractional order initial value problems across various domains. In view of the generalized ABM-PECE method, the numerical scheme for the proposed model (3.1) is given in the following form [23–26]:

$$\begin{aligned} U_{n+1} =& U_0 + \frac{h^{\zeta_1}}{\Gamma(\zeta_1+2)} \Big(\bar{\Omega}_P - \bar{\nu}_P U^p_{n+1} - \bar{\lambda}_1 \frac{U^p_{n+1} V^p_{n+1}}{N} \\ & - \bar{\lambda}_2 \frac{U^p_{n+1} Y^p_{n+1}}{N}\Big) + \frac{h^{\zeta_1}}{\Gamma(\zeta_1+2)} \sum_{j=0}^{n} \zeta_{1,j,n+1} \\ & \Big(\bar{\Omega}_P - \bar{\nu}_P U_j - \bar{\lambda}_1 \frac{U_j V_j}{N} - \bar{\lambda}_2 \frac{U_j Y_j}{N}\Big), \\ V_{n+1} =& V_0 + \frac{h^{\zeta_2}}{\Gamma(\zeta_2+2)} \Big(\bar{\lambda}_1 \frac{U^p_{n+1} V^p_{n+1}}{N} + \bar{\lambda}_2 \frac{U^p_{n+1} Y^p_{n+1}}{N} \end{aligned}$$

$$
\begin{aligned}
&- \left(\bar{\nu}_P + \bar{\rho} + \bar{\sigma}\right) V_{n+1}^p \Big) + \frac{h^{\zeta_2}}{\Gamma(\zeta_2+2)} \sum_{j=0}^{n} \zeta_{2,j,n+1} \\
&\left(\bar{\lambda}_1 \frac{U_j V_j}{N} + \bar{\lambda}_2 \frac{U_j Y_j}{N} - \left(\bar{\nu}_P + \bar{\rho} + \bar{\sigma}\right) V_j\right), \\
W_{n+1} =& W_0 + \frac{h^{\zeta_3}}{\Gamma(\zeta_3+2)} \left(\bar{\rho} V_{n+1}^p - \bar{\nu}_P W_{n+1}^p\right) \\
&+ \frac{h^{\zeta_3}}{\Gamma(\zeta_3+2)} \sum_{j=0}^{n} \zeta_{3,j,n+1} \left(\bar{\rho} V_j - \bar{\nu}_P W_j\right), \\
X_{n+1} =& X_0 + \frac{h^{\zeta_4}}{\Gamma(\zeta_4+2)} \left(\bar{\Omega}_T - \bar{\nu}_T X_{n+1}^p - \bar{\lambda}_3 \frac{X_{n+1}^p V_{n+1}^p}{N}\right) \\
&+ \frac{h^{\zeta_4}}{\Gamma(\zeta_4+2)} \sum_{j=0}^{n} \zeta_{4,j,n+1} \left(\bar{\Omega}_T - \bar{\nu}_T X_j - \bar{\lambda}_3 \frac{X_j V_j}{N}\right), \\
Y_{n+1} =& Y_0 + \frac{h^{\zeta_5}}{\Gamma(\zeta_5+2)} \left(\bar{\lambda}_3 \frac{X_{n+1}^p V_{n+1}^p}{N} - \bar{\nu}_T Y_{n+1}^p\right) \\
&+ \frac{h^{\zeta_5}}{\Gamma(\zeta_5+2)} \sum_{j=0}^{n} \zeta_{5,j,n+1} \left(\bar{\lambda}_3 \frac{X_j V_j}{N} - \bar{\nu}_T Y_j\right),
\end{aligned}
$$

where

$$
\begin{aligned}
U_{n+1}^p =& U_0 + \frac{1}{\Gamma(\zeta_1)} \sum_{j=0}^{n} \beta_{1,j,n+1} \\
&\left(\bar{\Omega}_P - \bar{\nu}_P U_j - \bar{\lambda}_1 \frac{U_j V_j}{N} - \bar{\lambda}_2 \frac{U_j Y_j}{N}\right), \\
V_{n+1}^p =& V_0 + \frac{1}{\Gamma(\zeta_2)} \sum_{j=0}^{n} \beta_{2,j,n+1} \\
&\left(\bar{\lambda}_1 \frac{U_j V_j}{N} + \bar{\lambda}_2 \frac{U_j Y_j}{N} - \left(\bar{\nu}_P + \bar{\rho} + \bar{\sigma}\right) V_j\right), \\
W_{n+1}^p =& W_0 + \frac{1}{\Gamma(\zeta_3)} \sum_{j=0}^{n} \beta_{3,j,n+1} \left(\bar{\rho} V_j - \bar{\nu}_P W_j\right), \\
X_{n+1}^p =& X_0 + \frac{1}{\Gamma(\zeta_4)} \sum_{j=0}^{n} \beta_{4,j,n+1} \left(\bar{\Omega}_T - \bar{\nu}_T X_j - \bar{\lambda}_3 \frac{X_j V_j}{N}\right), \\
Y_{n+1}^p =& Y_0 + \frac{1}{\Gamma(\zeta_5)} \sum_{j=0}^{n} \beta_{5,j,n+1} \left(\bar{\lambda}_3 \frac{X_j V_j}{N} - \bar{\nu}_T Y_j\right).
\end{aligned}
$$

7.3. Simulation results and discussions

In this work, the overall population is found to be N(0) = 61,000, the initial conditions are assumed as $U(0) = 10,000, V(0) = 8000, W(0) = 3000, X(0) = 30,000$, and $Y(0) = 10,000$, and the estimated parameter values are taken from the Table 1. Considering the above initial values and parameter values, we obtain the numerical simulation of the system (3.1) with classical and different fractional order values.

Figures 2 and 3 show the comparison result for the fractional ASFV model using FEM & ABM-PECE under the Caputo derivative at different values of ζ. The graphical representation clearly indicates that the analyzed fractional disease model provides a deeper and more insightful understanding of the disease behavior. The evolution of susceptible pigs versus days for various fractional orders of ζ is shown in Figure 2a. We note that once susceptible pigs enter the infected classes, their proportions gradually decline. Figure 2b shows the relationship between the infected pigs and days with various fractional orders ζ. As the value of ζ increases, a decrease in the infection rate among infected pigs is observed, which consequently results in a rise in the number of recovered pigs. Figure 3a shows the relationship between the recovered pigs in terms of days for different values of ζ. This leads us to the conclusion that the quantity of pigs retrieved rises with changing values of ζ.

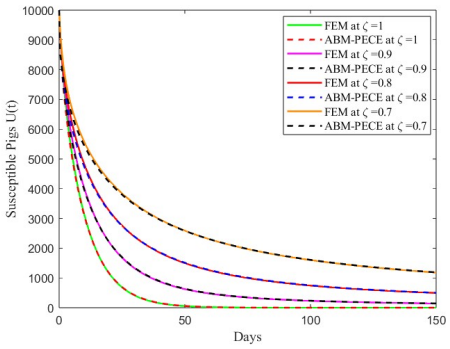

(a)

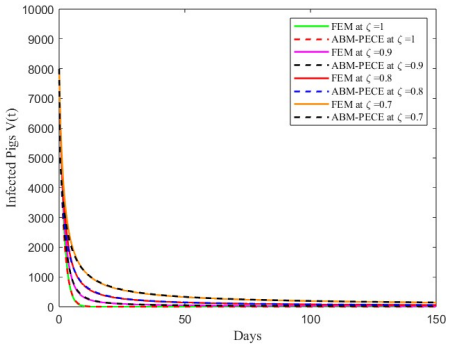

(b)

Figure 2. Comparison between the numerical results using FEM & ABM-PECE at different values of $\zeta = 1, 0.9, 0.8$ & 0.7.

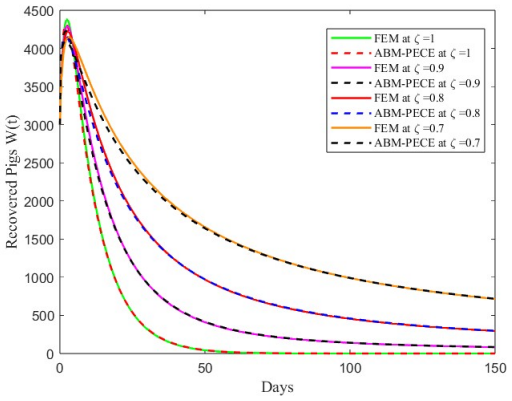

(a)

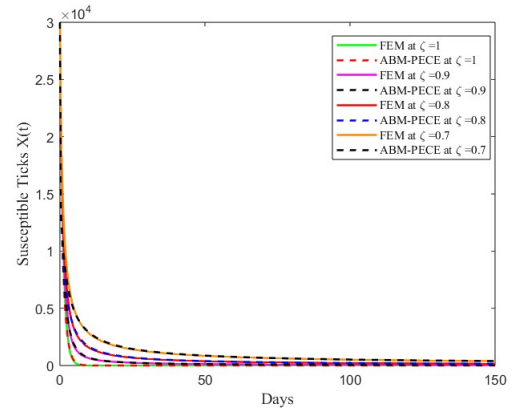

(b)

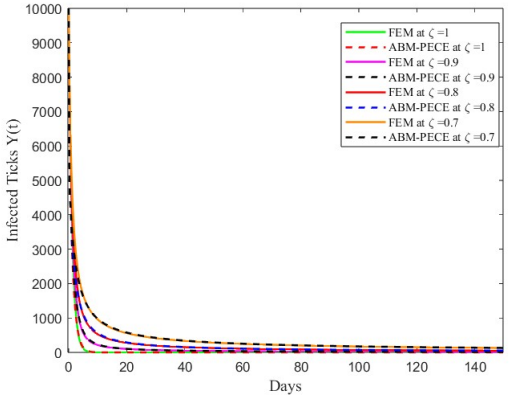

(c)

Figure 3. Comparison between the numerical results using FEM & ABM-PECE at different values of $\zeta = 1, 0.9, 0.8$ & 0.7.

Figure 3b illustrates the relationship between the behavior of susceptible ticks and days for various fractional orders of ζ. Moreover, the illustrated graphs reveal that as the value of ζ increases, there is a corresponding decrease in the infection rate of susceptible ticks. The dynamic behavior of infected ticks over days for different values of ζ is shown in Figure 3c, in which the proportion of infected ticks decreases with varying fractional orders of ζ. These graphical representations clearly showcase the enhanced performance of the Caputo version, which surpasses the results obtained from the classical version.

Table 3 shows that the Central Processing Unit (CPU) time for the ABM-PECE is lower than the FEM under the Caputo derivative at different values of ζ, see [27]. The computations are executed utilizing the MATLAB software, version R2021a, on a HP Desktop equipped with a 12th generation Intel Core i7 processor and 64 GB of RAM.

Table 3. CPU time in seconds.

ζ	CPUT for FEM	CPUT for ABM-PECE
$\zeta = 1$	0.0585	0.0251
$\zeta = 0.9$	0.0366	0.0247
$\zeta = 0.8$	0.0265	0.0241
$\zeta = 0.7$	0.0279	0.0250

8. Conclusions

In this study, to obtain a more comprehensive understanding of the virus dynamics, the classical compartmental model for the ASF virus between pigs and ticks was converted into a non-integer order model. On the basis of the Banach contraction principle, the model provided an unique solution. The existence of a positive solution for this model was proven using Krasnoselskii's fixed point theorem. UH and its generalised form were used to verify the stability of the Caputo sense model. The proposed model's numerical solution was obtained using the ABM-PECE method and compared to the FEM. According to Table 3 and the graphical findings, the ABM-PECE method was more effective than the FEM in describing biological results and had lower computational costs. As a result, the proposed CFO model was shown to have several significant features. It should be highlighted that the disease behavior of the ASFV model was better understood using

the CFO derivative than by employing variations of the integer order. Additionally, our numerical investigations contribute to a better understanding of the ASFV model, which can significantly enhance the optimization of prevention, targeting, and treatment strategies, and can ultimately lead to more effective disease management tools. In future research, we aim to expand this study by incorporating a time delay.

Use of Generative-AI tools declaration

The authors declare they have not used Artificial Intelligence (AI) tools in the creation of this article.

Conflict of interest

The authors declare that they have no conflicts of interest in this paper.

References

1. D. Baleanu, K. Diethelm, E. Scalas, J. J. Trujillo, *Fractional calculus: models and numerical methods*, World Scientific, 2012. https://doi.org/10.1142/8180
2. K. S. Miller, B. Ross, *An introduction to the fractional calculus and fractional differential equations*, Wiley-Interscience, 1993.
3. I. Petráš, *Fractional-order nonlinear systems: modeling, analysis and simulation*, Springer Berlin, Heidelberg, 2011. https://doi.org/10.1007/978-3-642-18101-6
4. S. Suganya, V. Parthiban, A mathematical review on Caputo fractional derivative models for COVID-19, *AIP Conf. Proc.*, **2852** (2023), 110003. https://doi.org/10.1063/5.0166410
5. M. B. Barongo, R. P. Bishop, E. M. Fèvre, D. L. Knobel, A. Ssematimba, A mathematical model that simulates control options for African swine fever virus (ASFV), *PloS One*, **11** (2016), 0158658. https://doi.org/10.1371/journal.pone.0158658
6. A. Kouidere, O. Balatif, M. Rachik, Analysis and optimal control of a mathematical modeling of the spread of African swine fever virus with a case study of South Korea and cost-effectiveness, *Chaos Soliton. Fract.*, **146** (2021), 110867. https://doi.org/10.1016/j.chaos.2021.110867
7. K. Yoon-seung, *S. Korea again reports african swine fever case since 2019*, 2020. Available from: `https://en.yna.co.kr/view/AEN20201009000700320`.
8. H. J. Kim, K. H. Cho, S. K. Lee, D. Y. Kim, J. J. Nah, H. J. Kim, et al., Outbreak of African swine fever in South Korea, 2019, *Transbound. Emerg. Dis.*, **67** (2020), 473–475. https://doi.org/10.1111/tbed.13483
9. R. Shi, Y. Li, C. Wang, Stability analysis and optimal control of a fractional-order model for African swine fever, *Virus Res.*, **288** (2020), 198111. https://doi.org/10.1016/j.virusres.2020.198111
10. Y. Zhou, *Basic theory of fractional differential equations*, World Scientific, 2023. https://doi.org/10.1142/13289
11. A. Aphithana, S. K. Ntouyas, J. Tariboon, Existence and Ulam-Hyers stability for Caputo conformable differential equations with four-point integral conditions, *Adv. Differ. Equ.*, **2019** (2019), 1–17. https://doi.org/10.1186/s13662-019-2077-5
12. A. Khan, H. Khan, J. F. Gómez-Aguilar, T. Abdeljawad, Existence and Hyers-Ulam stability for a nonlinear singular fractional differential equations with Mittag-Leffler kernel, *Chaos Soliton. Fract.*, **127** (2019), 422–427. https://doi.org/10.1016/j.chaos.2019.07.026
13. I. Ahmed, I. A. Baba, A. Yusuf, P. Kumam, W. Kumam, Analysis of Caputo fractional-order model for COVID-19 with lockdown, *Adv. Differ. Equ.*, **2020** (2020), 394. https://doi.org/10.1186/s13662-020-02853-0
14. E. Hincal, S. H. Alsaadi, Stability analysis of fractional order model on corona transmission dynamics, *Chaos Soliton. Fract.*, **143** (2021), 110628. https://doi.org/10.1016/j.chaos.2020.110628
15. M. A. Khan, A. Atangana, Modeling the dynamics of novel coronavirus (2019-nCov) with fractional derivative, *Alexandria Eng. J.*, **59** (2020), 2379–2389. https://doi.org/10.1016/j.aej.2020.02.033

16. K. Shah, F. Jarad, T. Abdeljawad, On a nonlinear fractional order model of dengue fever disease under Caputo-Fabrizio derivative, *Alex. Eng. J.*, **59** (2020), 2305–2313. https://doi.org/10.1016/j.aej.2020.02.022

17. P. Verma, S. Tiwari, A. Verma, Theoretical and numerical analysis of fractional order mathematical model on recent COVID-19 model using singular kernel, *Proc. Natl. Acda. Sci., India, Sect. A Phys. Sci.*, **93** (2023), 219–232. https://doi.org/10.1007/s40010-022-00805-9

18. A. Jajarmi, D. Baleanu, A new fractional analysis on the interaction of HIV with $CD4^+$ T-cells, *Chaos Soliton. Fract.*, **113** (2018), 221–229. https://doi.org/10.1016/j.chaos.2018.06.009

19. C. Li, F. Zeng, *Numerical methods for fractional calculus*, New York: Chapman and Hall/CRC, 2015. https://doi.org/10.1201/b18503

20. M. Z. Ullah, A. K. Alzahrani, D. Baleanu, An efficient numerical technique for a new fractional tuberculosis model with nonsingular derivative operator, *J. Taibah Univ. Sci.*, **13** (2019), 1147–1157. https://doi.org/10.1080/16583655.2019.1688543

21. M. Awais, F. S. Alshammari, S. Ullah, M. A. Khan, S. Islam, Modeling and simulation of the novel coronavirus in Caputo derivative, *Results Phys.*, **19** (2020), 103588. https://doi.org/10.1016/j.rinp.2020.103588

22. D. Baleanu, A. Jajarmi, M. Hajipour, On the nonlinear dynamical systems within the generalized fractional derivatives with Mittag–Leffler kernel, *Nonlinear Dyn.*, **94** (2018), 397–414. https://doi.org/10.1007/s11071-018-4367-y

23. F. Evirgen, Transmission of Nipah virus dynamics under Caputo fractional derivative, *J. Comput. Appl. Math.*, **418** (2023), 114654. https://doi.org/10.1016/j.cam.2022.114654

24. M. Helikumi, P. O. Lolika, Dynamics and analysis of COVID-19 disease transmission: the effect of vaccination and quarantine, *Math. Model. Control*, **3** (2023), 192–209. https://doi.org/10.3934/mmc.2023017

25. S. Paul, A. Mahata, S. Mukherjee, B. Roy, Dynamics of SIQR epidemic model with fractional order derivative, *Partial Differ. Equ. Appl. Math.*, **5** (2022), 100216. https://doi.org/10.1016/j.padiff.2021.100216

26. S. Paul, A. Mahata, S. Mukherjee, B. Roy, M. Salimi, A. Ahmadian, Study of fractional order SEIR epidemic model and effect of vaccination on the spread of COVID-19, *Int. J. Appl. Comput. Math.*, **8** (2022), 237. https://doi.org/10.1007/s40819-022-01411-4

27. N. H. Sweilam, S. M. Al-Mekhlafi, A. Almutairi, D. Baleanu, A hybrid fractional COVID-19 model with general population mask use: numerical treatments, *Alex. Eng. J.*, **60** (2021), 3219–3232. https://doi.org/10.1016/j.aej.2021.01.057

AIMS Press